Optical properties of human maxillary sinus mucosa and estimation of Methylene Blue diffusion coefficient in the tissue

Alexey N. Bashkatov*), Elina A. Genina*, Vyacheslav I. Kochubey*, Valery V. Tuchin*, Elena E. Chikina**, Anatoly B. Knyazev**, Oleg V. Mareev**
Institute of Optics and Biophotonics, and Optics Department of Saratov State University,
410012, 83 Astrakhanskaya str., Saratov, Russia
** Department of Otolaryngology of Saratov State Medical University,
410012, 112 B. Kazachya str., Saratov, Russia

ABSTRACT

The optical properties of human maxillary sinus mucosa were measured in the wavelength range 400-2000 nm. The measurements were carried out using the commercially available spectrophotometer with the integrating sphere. The inverse adding-doubling method has been used to determine the absorption and reduced scattering coefficients from the measurements. Diffusion of Methylene Blue in the mucous tissue has been studied *in vitro* and value of the diffusion coefficient of Methylene Blue in the tissue has been estimated at 20°C as $(4.77 \pm 2.9) \times 10^{-7}$ cm^2/sec.

Keywords: optical properties, absorption coefficient, reduced scattering coefficient, optical penetration depth, diffusion, Methylene Blue, otolaryngology, photodynamic therapy, acute maxillary sinusitis, chronic maxillary sinusitis

1. INTRODUCTION

Development of optical method in modern medicine in the areas of diagnostics, therapy and surgery has stimulated the investigation of optical properties of various biological tissues, since the efficacy of laser treatment depends on the photon propagation and fluence rate distribution within irradiated tissues. Examples of diagnostic use are the monitoring of blood oxygenation and tissue metabolism[1], laser Doppler flowmetry[2], pulse oximetry[3], detection of cancer by fluorescence[4] and spectrophotometric methods[5], and recently suggested various techniques for optical imaging[6,7]. Therapeutic uses include applications in laser surgery[8], laser angioplasty and ablation[9,10] and in photodynamic therapy[11,12]. For these applications, the knowledge of tissue optical properties is of great importance for interpretation and quantification of diagnostic data, and to predict light distribution and absorbed dose for therapeutic use. The knowledge of tissue optical properties is also necessary for the development of the novel optical technologies of photodynamic and photothermal therapy, optical tomography, optical biopsy, and etc. Numerous investigations related to determination of tissue optical properties are available, however the optical properties of many tissues have not been studied in a wide wavelength range.

Investigation of the mucous optical properties is necessary for light dosimetry at photodynamic therapy of bladder, colon, esophagus, stomach etc. The treatment of purulent maxillary sinusitis is an important problem in modern rhinology despite the wide application of surgical and pharmaceutical methods[13,14]. One of the new methods of treatment of this disease is photodynamic therapy of the mucous membrane of the maxillary sinus[13]. The optical properties of mucous tissues were shown by Müller and Roggan[15] for the wavelength 1064 nm. However, in a wide wavelength range the optical properties of mucous tissues have not been measured.

Development of the novel photodynamic methods includes knowledge of photosensitizers diffusion rate, choice of laser source and optimal conditions for the laser irradiation and delivering the photosensitizers into human tissue. Methylene Blue is very appropriate as a photosensitizer due to its biocompatibility and low cost. However, in spite of numerous investigations related to application of Methylene Blue in photodynamic therapy of different diseases[16-23], the Methylene Blue diffusion coefficient in epithelial tissues has not been estimated.

*) bash@optics.sgu.ru

Saratov Fall Meeting 2004: Optical Technologies in Biophysics and Medicine VI,
edited by Valery V. Tuchin, Proc. of SPIE Vol. 5771 (SPIE, Bellingham, WA, 2005)
1605-7422/05/$15 · doi: 10.1117/12.634835

The goal of this paper is to measure the absorption and reduced scattering coefficients of human mucous in the wavelength range from 400 to 2000 nm, and to investigate of the Methylene Blue diffusion in human mucous tissue and to estimate value of its diffusion coefficient.

2. PHYSICAL PROPERTIES AND STRUCTURE OF THE TISSUE

The mucous membrane plays a leading role in the physiology of the nose and paranasal sinuses[14,24]. It is covered with a pseudostratified epithelium, which consists of ciliated, columbar as well as short and long inserted epithelial cells. The membrane called basic divides epithelial and proper layers of the mucous tissue and consists of reticular fibrils, which are located in the interstitial homogeneous media. The membrane has not a constant thickness. In the case of hyperplasia of the mucous membrane, the membrane considerably thickens[25].

The proper layer of the mucous membrane is similar in structure to connective tissue, consisting of collagen and elastin fibrils. The interstitial fluid of the mucous membrane contains proteins and polysaccharides and is similar in composition to the interstitial fluid of the most of connective tissues. The proper layer of the mucous membrane consists of three sublayers. A subepithelial (or lymphoid) layer contains a great amount of leukocytes. In the intermediate sublayer of the proper layer, tubuloalveolar glands are contained. In the deep sublayer of the proper layer, venous plexuses are arranged, which consist of a surface network of smaller vessels and a deeper network of larger vessels. Normally, the total thickness of the mucous membrane varies from 0.1 to 0.5 mm[14,24]. In the presence of pathology (maxillary sinusitis, rhinitis, or other rhinological disease), the thickness of the mucous membrane considerably increases and can reach 2-3 mm[14]. It should be noted, that the proper layer of the mucous membrane is the main layer protecting against microorganisms causing infectious diseases[24]. The optical properties of the mucous membranes are mainly determined by the optical properties of the proper layer since this layer is much thicker than the epithelial layer.

3. METHOD FOR ESTIMATION OF METHYLENE BLUE DIFFUSION COEFFICIENT

Method of estimation of Methylene Blue (MB) diffusion coefficient is based on the time-dependent measurement of the tissue absorbance in the spectral range from 600 to 700 nm, which correspond to absorption bands of the dye. The transport of MB within the mucous tissue is described in the framework of free diffusion model. We assume that the following approximations are valid for the transport process:

1. Only concentration diffusion takes place; i.e., the flux of the dye into the tissue, at a certain point within the tissue sample, is proportional to the MB concentration at this point;
2. The diffusion coefficient is constant over the entire sample volume.

Geometrically the tissue sample is presented as a plane-parallel slab with a finite thickness. Since lateral sides of the experimental samples were fixed, the one-dimensional diffusion problem has been solved. The one-dimensional diffusion equation of the dye transport has the form

$$\frac{\partial C(x,t)}{\partial t} = D\frac{\partial^2 C(x,t)}{\partial x^2}, \tag{1}$$

where $C(x,t)$ is the MB concentration, g/ml; D is the MB diffusion coefficient, cm^2/s; t is time, in second, s; and x is the spatial coordinate, cm.

We also suppose that penetration of the MB into a tissue sample does not change the dye concentration in the external volume. Besides, due to geometry of the measurements, penetration of the MB into a tissue sample takes place from top surface of the tissue sample only. The corresponding boundary conditions are

$$C(0,t) = C_0 \quad \text{and} \quad \frac{\partial C(l,t)}{\partial x} = 0, \tag{2}$$

where C_0 is MB concentration in external solution, g/ml, and l is tissue sample thickness, cm.

The initial condition corresponds to the absence of MB inside the mucous tissue before the measurements,

$$C(x,0) = 0\,, \tag{3}$$

for all inner points of the tissue sample.

Solution of Eq. 1 for a slab with a thickness l at the moment t with boundary (Eq. 2) end initial (Eq. 3) conditions has the form

$$C(t) = C_0\left(1 - \frac{8}{\pi^2}\sum_{i=0}^{\infty}\frac{1}{(2i+1)^2}\exp\left(-(2i+1)^2\, t\,\frac{\pi^2}{4}\,D\Big/l^2\right)\right), \tag{4}$$

where $C(t)$ is the volume-averaged concentration of MB within tissue sample.

In a first-order approximation, Eq. 4 is reduced to the form

$$C(t) \approx C_0\left(1 - \exp\left(-t\pi D/l^2\right)\right). \tag{5}$$

For determination of MB diffusion coefficient in the mucous tissue the approach suggested by Mourant et al.[26] has been used. The method is based on the use of modified Lambert-Beer law and in this case, tissue absorbance can be determined as

$$A = \mu_a \sigma\rho + G\,, \tag{6}$$

where μ_a is absorption coefficient, ρ is source-detector distance, σ is differential factor of photon path-length, taking into account the lengthening of photon trajectories due to multiple scattering, and G is constant, defined by geometry of the experiment. To simplify calculations, $\rho\sigma$ can be replaced by parameter L which is defined by both absorption and scattering tissue properties, and source-detector distance. Since in this study the distance (290 μm) is commensurable with photon free path-length, parameter L is defined by tissue scattering properties only[27,28].

Penetration of MB into tissue is increasing the tissue absorbance in spectral range corresponding to absorption bands of the dye. Thus, the tissue absorbance measured in different time intervals can be determined as

$$A(t,\lambda) = A(t=0,\lambda) + \Delta\mu_a(t,\lambda)L\,, \tag{7}$$

where t is the time interval, λ is the wavelength, $\Delta\mu_a(t,\lambda) = \varepsilon(\lambda)C(t)$ is the absorption coefficient of MB within tissue, $\varepsilon(\lambda)$ is MB molar absorption coefficient, $C(t)$ is MB concentration in tissue, and $A(t=0,\lambda)$ is the tissue absorbance, measured in the initial moment.

Thus, the equation

$$\Delta A(t,\lambda) = A(t,\lambda) - A(t=0,\lambda) = \Delta\mu_a(t,\lambda)L = \varepsilon(\lambda)C_0\left(1 - \exp\left(-t\pi D/l^2\right)\right)L \tag{8}$$

can be used for calculation of the MB diffusion coefficient.

This set of equation represents the direct problem, i.e., describes the temporal evaluation of the absorbance of a tissue sample dependent on MB concentration within the tissue sample. Based on measurement of the evolution of the tissue absorbance, the reconstruction of the MB diffusion coefficient in mucous tissue has been carried out. The inverse problem solution has been obtained by minimization of the target function as

$$F(D) = \sum_{i=1}^{N_t}\left(A(D,t_i) - A^*(t_i)\right)^2, \tag{9}$$

where $A(D,t)$ and $A^*(t)$ are the calculated and experimental values of the time-dependent absorbance, respectively, and N_t is the number of time points obtained at registration of the temporal dynamics of the absorbance. To minimize the target function the Levenberg-Marquardt nonlinear least-squares-fitting algorithm described in detail by Press et al.[29] has been used. Iteration procedure repeats until experimental and calculated data are matched.

4. MATERIALS AND METHODS

The measurements have been performed *in vitro* with twenty samples of the mucous membrane of the maxillary sinuses, which was obtained from twenty patients with chronic maxillary sinusitis during the planned surgery. All tissue samples were kept in saline at room temperature about 20°C until spectroscopic measurements. The mucous tissue samples were measured during 2-3 hours after biopsy. Measurements of optical properties of the human mucous tissue have been carried out with ten the tissue samples. All the tissue samples has been cut into pieces with the area about 20×20 mm^2. For mechanical support, the tissue samples have been sandwiched between two glass slides. The thickness of each tissue sample has been measured with a micrometer in several points over the sample surface and averaged. Precision of the single measurement was ±50 μm.

The total transmittance and diffuse reflectance measurements have been performed in the 400-2000 nm wavelength range using the commercially available CARY-2415 ("Varian", Australia) spectrophotometer with an integrating sphere. Inner diameter of the sphere is 100 mm, size of the entrance port is 20×20 mm and diameter of the exit port is 16 mm. As a light source, a halogen lamp with filtering of the radiation in the studied spectral range has been used in the measurements. The diameter of incident light beam on the tissue sample is 3 mm. Scan rate is 2 nm/sec.

For processing the experimental data and determination of the optical properties of tissue, the inverse adding-doubling (IAD) method developed by Prahl et al.[30] has been used. The method is widely used in tissue optics for processing the experimental data of spectrophotometry with integrating spheres[31-36]. This method allows one to determine the absorption (μ_a) and the reduced scattering coefficients $(\mu_s' = \mu_s(1-g))$ of a tissue from the measured values of the total transmittance and the diffuse reflectance. Here μ_s is the scattering coefficient, and g is the anisotropy factor of scattering. In these calculations the anisotropy factor has been fixed as 0.9, since this value is typical for many tissues in the visible and NIR spectral ranges[37]. The main advantage of the IAD method in comparison with many other methods of solution of the radiative transfer equation is connected with its validation for the arbitrary ratio of the absorption and scattering coefficients[30]. The property of the IAD method becomes essentially important in the case of determination of the optical properties of tissues within strong absorption bands, when the values of the absorption and scattering coefficients become comparable. Other methods, for example, diffusion approximation[38-40] or Kubelka-Munk method[41-43], for their applicability require a fulfilment of the condition $\mu_a/\mu_s \ll 1$. The inverse Monte Carlo technique[44] can also be used for arbitrary ratio of μ_a and μ_s, but requires very extensive calculations. The main limitation of IAD method is connected with the possible loss of scattering radiation through lateral sides of a sample at calculations[45]. Loss of light through the sides of the sample and sample holder may erroneously increase the calculated value of the absorption coefficient. These losses depend on the physical size and geometry of the sample, i.e., the losses existing in the case, when the sizes of a sample do not exceed significantly the diameter of the incident beam. The size of the exit and the entrance ports of the integrating sphere are also important for errorless measurements of the total transmittance and the diffuse reflectance[45]. The tissue sample should completely cover the port in the integrating sphere, and the distance from the edge of irradiating beam on the sample to the edge of the port should be much larger than the lateral light propagation distance, which is determined as $1/(\mu_a + \mu_s')$. If this is not satisfied, then light will be lost out from the sides of the sample and the loss will be attributed to absorption, and so the absorption coefficient will be overestimated. These requirements have been met in our experiments, since maximal size of the sphere port does not exceed 20 mm, while the minimal size of the tissue samples is 20 mm. In addition, using the absorption and the reduced scattering coefficients of the investigated tissues presented below, in the next section, we calculated the lateral light propagation distance. For the mucous tissue, the value is equal to 2.2 mm for the wavelength 1284 nm. Taking into account the diameter of the incident beam (3 mm), minimal size of a tissue sample has to be larger than 7.5 mm that was satisfied for each tissue sample under study. It is seen, that the lateral light propagation distance is smaller than the distance from the edge of the irradiating beam on the sample to the sample port edge. Besides, Pickering et al.[45] reported that area of tissue sample has to be smaller than the area of the inner surface of the integrating sphere. This requirement has also been met in our experiments, since the area of the inner surface of integrating sphere used in the measurements was 314.16 cm^2, while the area of any tissue sample does not exceed 5.0 cm^2.

Calculation of tissue optical properties was performed for each wavelength point. The algorithm consists of the following steps: (a) the estimation of a set of optical properties; (b) the calculation of the reflectance and transmittance with the adding-doubling iterative method; (c) the comparison of the calculated with the measured values of the reflectance and the transmittance; (d) iteration of the above steps until a match (within the specified acceptance margin) is reached. With this iterative process the set of optical properties that yields the closest match to the measured values of reflectance and transmittance are taken as the optical properties of the tissue.

In this study, aqueous solution of Methylene Blue with concentration 1 g/L has been used. The measurements of MB diffusion coefficient have been performed with ten samples of human mucous tissue obtained from ten patients with chronic maxillary sinusitis. The measurements have been performed in the spectral range 500-1000 nm using a commercially available optical multichannel spectrometer LESA-5 (BioSpec, Russia) with fiber-optical probe at room temperature about 20°C. The scheme of the experimental setup is shown in Fig. 1.

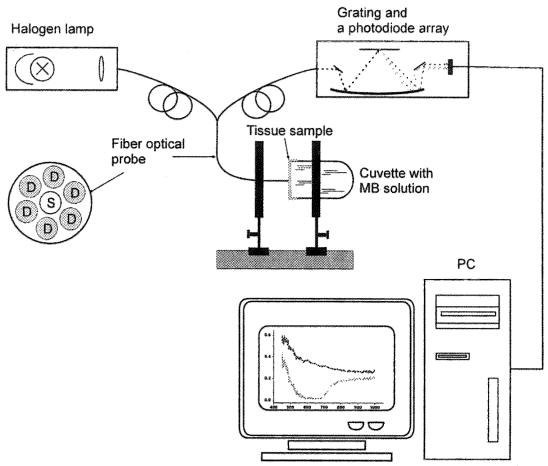

Fig. 1. Experimental setup for measurements of the mucous tissue reflectance spectra

The fiber-optical probe consists of the seven optical fibers. All fibers had 200 μm core diameter and a numerical aperture of 0.22. The central fiber delivers incident light to the tissue surface and the six fibers (the fibers are placed around the central fiber) collected reflected light. Distance between the delivering and receiving fibers is 290 μm. As a reference a white slab $BaSO_4$ with a smooth surface has been used. For the spectrophotometric measurements each tissue sample is fixed on the special cuvette with solution of MB. Dye solution penetration into a tissue sample was provided only through the outward surface of the sample that modeled real conditions of photodynamic procedure. Measured reflectance spectra have been recalculated in absorbance spectra with the relation

$$A(\lambda) = -\ln(R(\lambda)). \tag{10}$$

5. RESULTS AND DISCUSSION

Figure 2 shows the spectra of the total transmittance and the diffuse reflectance of human mucous tissue sample, measured in the spectral range from 400 to 2000 nm. In the visible spectral range the form of the presented spectra is defined by the absorption bands of blood of the mucous tissue and the spectral dependence of scattering coefficient of the tissue. In the infrared spectral range, absorption bands of water of interstitial matrix define the form of the spectra.

Figures 3 and 4 show the spectra of the absorption and reduced scattering coefficients calculated by the inverse adding-doubling method from the experimentally measured diffuse reflectance and total transmittance. Figure 3 shows the absorption spectrum of the mucous tissue in the spectral range from 400 to 2000 nm. The vertical lines indicate the standard deviation values (*SD*), which is determined as: $SD = \sqrt{\sum_{i=1}^{N}\left(\overline{\mu}_a - \mu_{ai}\right)^2 \Big/ n(n-1)}$, where n = 10 is number of

the measured tissue samples, μ_{ai} is the absorption coefficient of each sample, and $\overline{\mu}_a$ is the mean value of the absorption coefficient for each wavelength, which is calculated as $\sum_{i=1}^{N} \mu_{ai} \Big/ n$. In the spectrum absorption bands of blood oxyhaemoglobin (415, 540 and 575 nm[46]) and water (1450 and 1930 nm[47,48]) are clearly seen. The absorption bands of water located at 976 and 1197 nm[47,48] are considerably less observed. Absorption of water in visible spectral range is negligible[49].

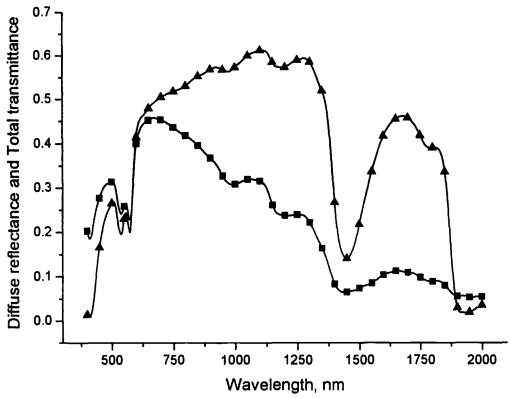

Fig. 2. The diffuse reflectance and total transmittance spectra of human mucous tissue sample. Symbols correspond to the experimental data. The squares correspond to the diffuse reflectance and the up triangles correspond to the total transmittance. Thickness of the sample is 1.5±0.1 mm.

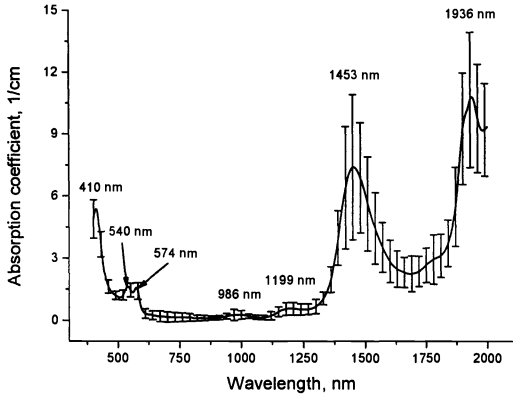

Fig. 3. The wavelength dependence of the absorption coefficients μ_a of human mucous tissue was calculated using IAD method. The solid line corresponds to the averaged experimental data and the vertical lines show the standard deviation values.

Recently, optical properties of mucous tissue have been presented by Müller and Roggan[15] and Shah et al.[50], for the wavelength 1064 nm. For this wavelength, the absorption coefficient of mucous layer of bladder, colon, esophagus, stomach[15] and tonsillar[50] are 0.7, 2.7, 1.1 and 2.8 cm^{-1} and 0.39 cm^{-1}, respectively. For this wavelength we obtained $\mu_a = 0.14 \pm 0.1$ cm^{-1}.

Figure 4 presents the spectral dependence of the reduced scattering coefficient of the mucous tissue. This dependence was obtained by averaging of the spectra of the reduced scattering coefficient of the ten samples of the mucous tissue.

The vertical lines show standard deviation values. It is clearly seen that with increase of wavelength, the reduced scattering coefficient decreases smoothly, which corresponds to the general spectral behaviour of the scattering characteristics of biological tissues[37,51-53]. However, in the range of the strong absorption bands (415, 1450 and 1930 nm), the shape of the scattering spectrum deviates from a monotonic dependence. At the same time, in the range of the water absorption bands with maximums at 976 and 1197 nm the effect is not observed. For the wavelength 1064 nm Müller and Roggan[15] and Shah et al.[50] reported that the reduced scattering coefficients of mucous layer of bladder, colon, esophagus, stomach[15] and tonsillar[50] are 1.1, 3.5, 11.6 and 65.9 cm^{-1} and 5.2 cm^{-1}, respectively. For this wavelength we obtained $\mu_s' = 5.51 \pm 0.6$ cm^{-1}.

In the spectral range 600-1500 nm for many tissues the reduced scattering coefficient decreases with the wavelength in accordance with a power law $\mu_s'(\lambda) = a\lambda^{-w}$ [51-53], where parameter a is defined by concentration of tissue scatterers. The wavelength exponent w characterizes the mean size of the tissue scatterers and defines spectral behaviour of the reduced scattering coefficient. Both the parameter a and the wavelength exponent w are defined by the ratio of refractive indices of the scatterers and environment medium. Figure 4 shows approximation of the wavelength dependence of the reduced scattering coefficient by the power law $\mu_s'(\lambda) = 443742.6\lambda^{-1.62}$, where λ is wavelength, nm. In the figure it is seen, that in the spectral range from 600 to 1300 nm this power law well approximates the experimental data in contrast to the data in the spectral ranges 400-600 nm and 1300-2000 nm. Obtained in this study the value of the wavelength exponent ($w = 1.62$) is typical for many tissues. For estimation of the mean size of scatterers of the mucous tissue, the spectroturbidimetric method, described in Ref. 54, has been used. In assumption that refractive indices of the tissue scatterers and interstitial fluid are 1.45 and 1.36[37,52,53], respectively, the corresponding estimated mean diameter of the scatterers is 0.3 μm. Taking into account this value and the structure of the tissue, we can assume that the main scatterers of the tissue are mitochondria and leukocytes. At the same time, collagen and elastin fibrils of the proper layer of the mucous membrane also contribute to the scattering properties of the tissue, especially in the short-wavelength range of spectrum.

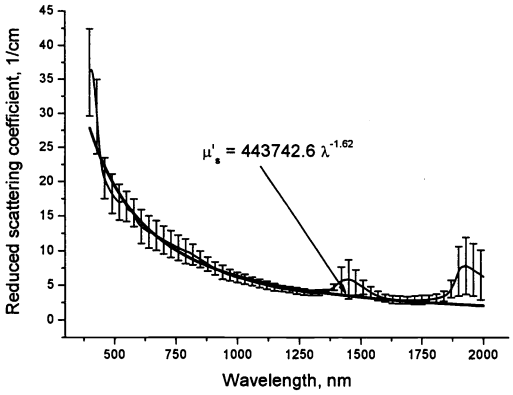

Fig. 4. The spectral dependence of the reduced scattering coefficient μ_s' of human mucous tissue calculated using IAD method and its approximation by power law. The vertical lines show the standard deviation values.

The deviation of the spectrum of the reduced scattering coefficient from a monotonic dependence can be explained by increase of the real part of complex refractive index of the tissue scatterers due to anomalous light dispersion. The increase of the imaginary part of the refractive index produces significant decrease of the anisotropy factor g, which, together with the scattering coefficient μ_s of a tissue, forms the tissue reduced scattering coefficient $\mu_s' = \mu_s(1-g)$. In Refs. 55 and 56 it was experimentally shown that in the range of water absorption bands, with maximum at 1450 and 1930 nm, significant decreasing the anisotropy factor is observed that produces increase of the reduced scattering coefficient and appearance of bands in its spectrum. Note that the degree of decrease of the anisotropy factor in the range of absorption bands is proportional to the intensity of the absorption bands. The tissue scattering coefficient in the range

of the absorption bands is decreased only slightly[55,56]. Such behaviour is explained by anomalous light dispersion, since within an absorption band the real part of refractive index corresponding to the short-wavelength wing of the absorption band goes down, and at the long-wavelength wing it goes up. Due to the fact the significant decrease of the anisotropy factor and the scattering coefficient within the absorption band should be observed. This was confirmed by Faber et al.[57], who calculated the wavelength dependencies of the scattering coefficient and the anisotropy factor of blood taking into account the spectral dependence of the real and imaginary parts of the complex refractive index of haemoglobin. The data presented in figure 4 are well explained using early discussed concept of anomalous light dispersion. In figure 3 one can see, that in the spectral range 600-1400 nm the absorption of mucous tissue is small. Hence, the scattering properties of the tissue are defined only by the real part of complex refractive index and the reduced scattering coefficient decreases rather monotonically with the wavelength. In the spectral range 1400-2000 nm the strong absorption bands of water is observed (see figure 3). The presence of the strong absorption bands leads to the fact that the scattering properties are formed not only under influence of the real, but also the imaginary part of a complex refractive index of the scattering centres, that produces increasing of the reduced scattering coefficient in the given spectral region with strong enough peaks in the range of the absorption bands. The scattering properties of the tissue in this wavelength range are defined by the real part of refractive index of water which have complex behaviour due to anomalous light dispersion and background scattering, which is defined by the light scattering on the tissue matrix which contained the blood capillaries and reticular fibrils. The background scattering decreases with the wavelength in accordance with a power law. In the spectral range 400-600 nm blood erythrocytes have a contribution in the mucous scattering spectrum, both due to their absorption and scattering properties[58]. The reduced scattering coefficient of whole blood decreases significantly within the absorption bands[59], thus the reduced scattering coefficient of adipose tissue decreases as well.

The depth penetration of light into a biological tissue is an important parameter for the correct determination of the irradiation dose in photothermal and photodynamic therapy of various diseases[37]. Estimation of the light penetration depth δ can be performed with the relation[56]:

$$\delta = 1/\sqrt{3\mu_a\left(\mu_a + \mu_s'\right)}\,. \tag{11}$$

Calculation of the optical penetration depth has been performed with the absorption and the reduced scattering coefficient values presented in figures 3 and 4, respectively, and the result presented in figure 5.

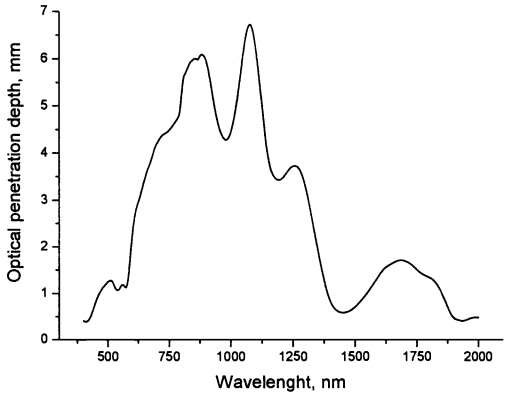

Fig. 5. The optical penetration depth δ of light into human mucous tissue over the wavelength range from 400 to 2000 nm

From figure 5 it is seen that, in dependence on the wavelength, the penetration depth varies considerably. The depth is maximal in the spectral ranges 800-900 nm and 1000-1100 nm, where the optical radiation penetrates to depths of up to 6-6.5 mm, which significantly exceeds the thickness of the mucous membrane both in the normal and in the pathological state. In the range of wavelengths of a He-Ne (633 nm) and a diode (660 nm) lasers, which are most frequently used in photodynamic therapy[37], the penetration depth amounts to 3-3.5 mm, which also exceeds the thickness of the mucous membrane.

Figures 6 and 7 show the wavelength and the temporal dependencies of MB absorbance. Figure 6 presents the dye absorbance measured for different time intervals. From the figure it is well seen that in the spectral range from 600 to 700 nm,

corresponding to absorption bands of MB, absorbance of the mucous tissue is increased during MB penetration into the tissue. In the figure also see, that shape of the spectrum is different for different moments. At the initial moment only one peak with maximum at 669 nm is seen, that corresponds to monomer form of the Methylene Blue molecules. During penetration of the MB solution into the tissue the interaction between MB molecules and tissue components are taking place. As a sequence of the interaction the MB molecules form dimmers, and two peaks with maximums at 609 and 669 nm in the spectrum presented in figure 6 are observed.

In the figure it is also seen that the penetration of the dye into the tissue does not change scattering properties of the skin. It is caused from the absence of the change in the absorbance spectra in the range 750-1000 nm, where MB has not the absorption bands, and the form of the absorbance spectra is determined by spectral dependence of scattering coefficient.

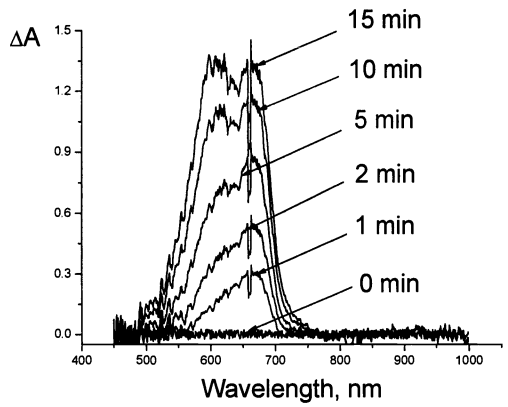

Fig. 6. The dye absorbance measured for different time intervals

Figure 7 presents the calculated and measured dynamics of dye absorbance for different wavelengths. From the figure it is seen, that the optimal staining time was about 30 min after staining was finished and the change of the absorbance was not observed. On the basis of measurement of the temporal evolution of the absorbance, the reconstruction of the MB diffusion coefficient in the mucous tissue has been carried out. Taking into account thickness of the skin samples diffusion coefficient of MB was estimated from analysis of experimental curves. To minimize a target function the Levenberg-Marquardt nonlinear least-squares-fitting algorithm has been used. Calculations were made for ten wavelengths in the range 600-700 nm for each samples and obtained values were averaged. The mean value of the diffusion coefficient is $(4.77 \pm 2.9) \times 10^{-7}$ cm^2/sec.

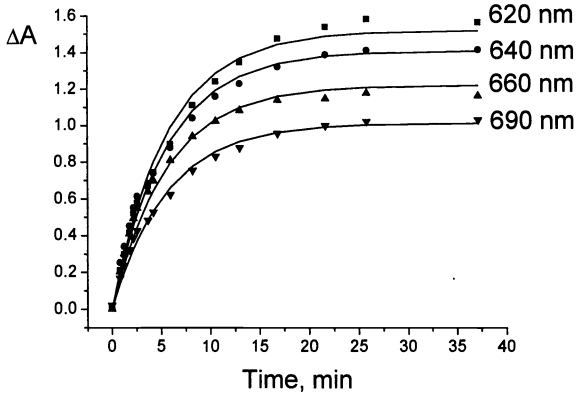

Fig. 7. Time-dynamics of the dye absorbance calculated for different wavelengths(solid lines) in comparison with experimental data (symbols)

6. CONCLUSION

The reduced scattering and the absorption coefficients of the human mucous tissue *in vitro* have been determined over the wavelength range 400-2000 nm using the integrating sphere technique and the inverse adding-doubling method. In this spectral range the absorption bands of oxyhaemoglobin and water with maxima at 415, 540, 575, 976, 1197, 1450, and 1930 nm are observed. For human mucous tissue in the spectral range from 400 to 2000 nm the reduced scattering coefficient decreases with the wavelength, but in the range of the strong absorption bands with maximums at 415, 1450 and 1930 nm the reduced scattering coefficient increases due to anomalous light dispersion. In the spectral range from 600 to 1300 nm the power law $\mu_s'(\lambda) = 443742.6\lambda^{-1.62}$ well approximates the experimental data. For this tissue the optical penetration depth has also been estimated. The effect of deviation of wavelength dependence of the reduced scattering coefficient of power law dependence in the spectral range 1300-2000 nm, can be explained by the strong influence of the imaginary part of the complex refractive index of scatterers. In the spectral range 400-600 nm the deviation has been explained by the influence of blood erythrocytes, which have contributed to the scattering and absorption spectra of the mucous tissue.

Based on temporal dependence of the tissue absorbance and the model presented, Methylene Blue diffusion coefficient in the mucous tissue at 20°C has been estimated as $(4.77 \pm 2.9) \times 10^{-7}$ cm^2/s.

The presented results can be used for the development of the optical technologies and can be helpful in photodynamic and photothermal therapy.

ACKNOWLEDGMENTS

The research described in this publication has been made possible, in part, by grant REC-006/SA-006-00, Annex N. 07 "Nonlinear Dynamics and Biophysics" of U.S. Civilian Research and Development Foundation for the Independent States of the Former Soviet Union (CRDF) and the Russian Ministry of Science and Education; the Russian Federation President's grant N 25.2003.2 "Supporting of Scientific Schools" and grant "Leading Research-Educational Teams" N 2.11.03 of the Russian Ministry of Science and Education. The authors thank Dr. S.V. Eremina (Department of English and Intercultural Communication of Saratov State University) for the help in manuscript translation to English.

REFERENCES

1. T. Hamaoka, T. Katsumura, N. Murase, S. Nishio, T. Osada, T. Sako, H. Higuchi, Y. Kurosawa, T. Shimomitsu, M. Miwa, B. Chance, "Quantification of ischemic muscle deoxygenation by near infrared time-resolved spectroscopy," *J. Biomed. Opt.*, **5**, 102-105, 2000.
2. V.G. Kolinko, F.F.M. de Mul, J. Greve, A.V. Priezzhev, "Feasibility of picosecond laser-Doppler flowmetry provides basis for time-resolved Doppler tomography of biological tissues," *J. Biomed. Opt.*, **3**, 187-190, 1998.
3. A. Zourabian, A. Siegel, B. Chance, N. Ramanujan, M. Rode, D.A. Boas, "Trans-abdominal monitoring of fetal arterial blood oxygenation using pulse oximetry," *J. Biomed. Opt.*, **5**, 391-405, 2000.
4. C.S. Betz, M. Mehlmann, K. Rick, H. Stepp, G. Grevers, R. Baumgartner, A. Leunig, "Autofluorescence imaging and spectroscopy of normal and malignant mucosa in patients with head and neck cancer," *Lasers Surg. Med.*, **25**, 323-334, 1999.
5. I.J. Bigio, S.G. Bown, G. Briggs, C. Kelley, S. Lakhani, D. Pickard, P.M. Ripley, I.G. Rose, C. Saunders, "Diagnosis of breast cancer using elastic-scattering spectroscopy: preliminary clinical results," *J. Biomed. Opt.*, **5**, 221-228, 2000.
6. M.E. Arnoldussen, D. Cohen, G.H. Bearman, W.S. Grundfest, "Consequences of scattering for spectral imaging of turbid biological tissue," *J. Biomed. Opt.*, **5**, 300-306, 2000.
7. S.G. Demos, R. Gandour-Edwards, R. Ramsamooj, R. White, "Spectroscopic detection of bladder cancer using near-infrared imaging techniques," *J. Biomed. Opt.*, **9**, 767-771, 2004.
8. B.A. Buscher, T.O. McMeekin, D. Goodwin, "Treatment of leg telangiectasia by using a long-pulse dye laser at 595 nm with and without dynamic cooling device," *Lasers Surg. Med.*, **27**, 171-175, 2000.
9. G.S. Abela, E.E. Hage-Korban, T. Tomaru, G.R. Barbeau, O.G. Abela, S.E. Friedl, "Vascular procedures that thermo-coagulate collagen reduce local platelet deposition and thrombus formation: laser and laser-thermal versus balloon angioplasty," *Lasers Surg. Med.*, **29**, 455-463, 2001.

10. T.S. Dietlein, P.C. Jacobi, G.K. Krieglstein, "Erbium:YAG laser trabecular ablation (LTA) in the surgical treatment of glaucoma," *Lasers Surg. Med.,* **23**, 104-110, 1998.
11. V.V. Tuchin, E.A. Genina, A.N. Bashkatov, G.V. Simonenko, O.D. Odoevskaya, G.B. Altshuler, "A pilot study of ICG laser therapy of *acne vulgaris*: photodynamic and photothermolysis treatment," *Lasers Surg. Med.,* **33**, 296-310, 2003.
12. E.A. Genina, A.N. Bashkatov, G.V. Simonenko, O.D. Odoevskaya, V.V. Tuchin, G.B. Altshuler, "Low-intensity indocyanine-green laser phototherapy of acne vulgaris: Pilot study," *J. Biomed. Opt.,* **9**, 828-834, 2004.
13. A.N. Nasedkin, V.G. Zenger, S.V. Grachev, V.M. Isaev, E.I. Prokof'eva, V.N. Selin, I.V. Leskov, A.V. Reshetnikov, I.D. Zalevskiy, S.E. Goncharov, Yu.V. Kemov, "The experience of application of photodynamic therapy for treatment acute and chronic purulent antritis," *Russian Rhinology,* **2**, 116, 2002 (in Russian).
14. G.Z. Piskunov, S.Z. Piskunov, *Clinical Rhinology* (Moscow: Miklon), 2002 (in Russian).
15. *Laser–Induced Interstitial Thermotherapy* PM25, G. Müller, A. Roggan, Eds., Washington: SPIE Press, 1995.
16. K. Konig, H. Meyer, "Photodynamic activity of Methylene Blue," *Akt. Dermatol.*, **19**, 195-198, 1993.
17. K. Orth, A. Ruck, A. Stanescu, H.G. Beger, "Intraluminal treatment of inoperable oesophageal tumours by intralesional photodynamic therapy with methylene blue," *Lancet*, **345**, 519-520, 1995.
18. C.E. Millson, M. Wilson, A.J. MacRobert, S.G. Bown, "Ex-vivo treatment of gastric *Helicobacter* infection by photodynamic therapy," *J. Photochem. Photobiol. B.*, **32**, 59-65, 1996.
19. M.S. Ismail, U. Torsten, C. Dressler, J.E. Diederichs, S. Huske, H. Weitzel, H.-P. Berlien, "Photodynamic therapy of malignant ovarian tumours cultivated on CAM," *Lasers Med. Sci.,* **14**, 91-96, 1999.
20. K. Orth, G. Beck, F. Genze, A. Ruck, "Methylene blue mediated photodynamic therapy in experimental colorectal tumors in mice," *J. Photochem. Photobiol. B.*, **57**, 186-192, 2000.
21. B. Zeina, J. Greenman, W.M. Purcell, B. Das, "Killing of cutaneous microbial species by photodynamic therapy," *Br. J. Dermatology*, **144**, 274-278, 2001.
22. I.D. Botterill, P.M. Sagar, "Intra-dermal methylene blue, hydrocortisone and lignocaine for chronic, intractable pruritus ani," *Colorectal Disease* **4**, 144-146, 2002.
23. M.C. Teichert, J.W. Jones, M.N. Usacheva, M.A. Biel, "Treatment of oral candidiasis with methylene blue-mediated photodynamic therapy in an immunodeficient murine model," *Oral Surgery, Oral Medicine, Oral Pathology, Oral Radiology & Endodontics* **93**, 155-160, 2002.
24. G.Z. Piskunov, S.Z. Piskunov, *Diagnostics and medical treatment of inflammatory processes of the mucous membrane of nose and maxillary sinuses,* Voronezh: Voronezh State University Press, 1991 (in Russian).
25. M.A. Zavaliy, A.G. Balabantsev, A.K. Zagorul'ko, T.G. Filonenko, "State of ciliary epithelium of patients with the chronic purulent sinusitis," *Russian Rhinology,* **2**, 19-22, 2002 (in Russian).
26. J.R. Mourant, T.M. Johnson, G. Los, I.J. Bigio, "Non-invasive measurement of chemotherapy drug concentrations in tissue: preliminary demonstrations of *in vivo* measurements," *Phys. Med. Biol.*, **44**, 1397-1417 1999.
27. J.R. Mourant, I.J. Bigio, D.A. Jack, T.M. Johnson, H.D. Miller, "Measuring absorption coefficients in small volumes of highly scattering media: source-detector separations for which path lengths do not depend on scattering properties," *Appl. Opt.*, **36**, 5655-5661, 1997.
28. F. Bevilacqua, C. Depeursinge, "Monte Carlo study of diffuse reflectance at source-detector separations close to one transport mean free path," *J. Opt. Soc. Am. A.*, **16**, 2935-2945, 1999.
29. W.H. Press, S.A. Tuekolsky, W.T. Vettering, B.P. Flannery, *Numerical Recipes in C: The Art of Scientific Computing.* Cambridge University Press, Cambridge, UK, 1992.
30. S.A. Prahl, M.J.C. van Gemert, A.J. Welch, "Determining the optical properties of turbid media by using the adding-doubling method," *Appl. Opt.,* **32**, 559-568, 1993.
31. T.L. Troy, S.N. Thennadil, "Optical properties of human skin in the near infrared wavelength range of 1000 to 2200 nm," *J. Biomed. Opt.,* **6**, 167-176, 2001.
32. B. Nemati, H.G. Rylander III, A.J. Welch, "Optical properties of conjunctiva, sclera, and the ciliary body and their consequences for transscleral cyclophotocoagulation," *Appl. Opt.,* **35**, 3321-3327, 1996.
33. J.F. Beek, P. Blokland, P. Posthumus, M. Aalders, J.W. Pickering, H.J.C.M. Sterenborg, M.J.C. van Gemert, "*In vitro* double-integrating-sphere optical properties of tissues between 630 and 1064 nm," *Phys. Med. Biol.,* **42**, 2255-2261, 1997.
34. D.K. Sardar, M.L. Mayo, R.D. Glickman, "Optical characterization of melanin," *J. Biomed. Opt.,* **6**, 404-411, 2001.

35. A.N. Bashkatov, E.A. Genina, V.I. Kochubey, V.V. Tuchin, "Estimation of wavelength dependence of refractive index of collagen fibers of scleral tissue," *Proc.* SPIE, **4162,** 265-268, 2000.
36. A.N. Bashkatov, E.A. Genina, I.V. Korovina, V.I. Kochubey, Yu.P. Sinichkin, V.V. Tuchin, "*In vivo* and *in vitro* study of control of rat skin optical properties by acting of osmotical liquid," *Proc.* SPIE, **4224,** 300-311, 2000.
37. V.V. Tuchin, *Tissue Optics: Light Scattering Methods and Instruments for Medical Diagnosis,* Vol. TT38, Washington: SPIE Press, 2000.
38. T.J. Farrell, M.S. Patterson, B.C. Wilson, "A diffusion theory model of spatially resolved, steady-state diffuse reflectance for the noninvasive determination of tissue optical properties in vivo," *Med. Phys.,* **19,** 879-888, 1992.
39. J.S. Dam, P.E. Andersen, T. Dalgaard, P.E. Fabricius, "Determination of tissue optical properties from diffuse reflectance profiles by multivariate calibration," *Appl. Opt.,* **37**, 772-778, 1998.
40. F. Bevilacqua, D. Piguet, P. Marquet, J.D. Gross, B.J. Tromberg, C. Depeursinge, "*In vivo* local determination of tissue optical properties: applications to human brain," *Appl. Opt.,* **38**, 4939-4950, 1999.
41. D.W. Ebert, C. Roberts, S.K. Farrar, W.M. Johnston, A.S. Litsky, A.L. Bertone, "Articular cartilage optical properties in the spectral range 300-850 nm," *J. Biomed. Opt.,* **3**, 326-333, 1998.
42. S.K. Farrar, C. Roberts, W.M. Johnston, P.A. Weber, "Optical properties of human trabecular meshwork in the visible and near-infrared region," *Lasers Surg. Med.,* **25**, 348-362, 1999.
43. W.E. Vargas, "Inversion methods from Kubelka-Munk analysis," *J. Opt. A: Pure Appl. Opt.,* **4,** 452-456, 2002.
44. I.V. Yaroslavsky, A.N. Yaroslavsky, T. Goldbach, H.-J. Schwarzmaierm, "Inverse hybrid technique for determining the optical properties of turbid media from integrating-sphere measurements," *Appl. Opt.,* **35**, 6797-6809, 1996.
45. J.W. Pickering, S.A. Prahl, N. van Wieringen, J.F. Beek, H.J.C.M. Sterenborg, M.J.C. van Gemert, "Double-integrating-sphere system for measuring the optical properties of tissue," *Appl. Opt.,* **32**, 399-410, 1993.
46. S.A. Prahl, *Optical absorption of hemoglobin,* http://www.omlc.ogi.edu/spectra/, 1999.
47. L. Kou, D. Labrie, P. Chylek, "Refractive indices of water and ice in the 0.65-2.5μm spectral range," *Appl. Opt.,* **32**, 3531-3540, 1993.
48. K.F. Palmer, D. Williams, "Optical properties of water in the near infrared," *J. Opt. Soc. Am.,* **64**, 1107-1110, 1974.
49. R.C. Smith, K.S. Baker, "Optical properties of the clearest natural waters (200-800nm)," *Appl. Opt.,* **20**, 177-184, 1981.
50. R.K. Shah, B. Nemati, L.V. Wang, S.M. Shapshay, "Optical-thermal simulation of tonsillar tissue irradiation," *Lasers Surg. Med.,* **28**, 313-319, 2001.
51. J.R. Mourant, T. Fuselier, J. Boyer, T.M. Johnson, I.J. Bigio, "Predictions and measurements of scattering and absorption over broad wavelength ranges in tissue phantoms," *Appl. Opt.,* **36**, 949-957, 1997.
52. J.M. Schmitt, G. Kumar, "Optical scattering properties of soft tissue: a discrete particle model," *Appl. Opt.,* **37**, 2788-2797, 1998.
53. R.K. Wang, "Modelling optical properties of soft tissue by fractal distribution of scatterers," *J. Modern Opt.,* **47**, 103-120, 2000.
54. S.Yu. Shchyogolev, "Inverse problems of spectroturbidimetry of biological disperse systems: an overview," *J. Biomed. Opt.,* **4,** 490-503, 1999.
55. Y. Du, X.H. Hu, M. Cariveau, G.W. Kalmus, J.Q. Lu, "Optical properties of porcine skin dermis between 900 nm and 1500 nm," *Phys. Med. Biol.,* **46**, 167-181, 2001.
56. J.-P. Ritz, A. Roggan, C. Isbert, G. Muller, H. Buhr, C.-T. Germer, "Optical properties of native and coagulated porcine liver tissue between 400 and 2400 nm," *Lasers Surg. Med.,* **29**, 205-212, 2001.
57. D.J. Faber, M.C.G. Aalders, E.G. Mik, B A Hooper, M.J.C. van Gemert, T.G. van Leeuwen, "Oxygen saturation-dependent absorption and scattering of blood," *Phys. Rev. Lett.,* **93**, 028102-1-028102-4, 2004.
58. A. Roggan, M. Friebel, K. Dorschel, A. Hahn, G. Muller, "Optical properties of circulating human blood in the wavelength range 400-2500 nm," *J. Biomed. Opt.,* **4**, 36-46, 1999.
59. A.N. Bashkatov, D.M. Zhestkov, E.A. Genina, V.V. Tuchin, "Immersion clearing of human blood in visible and near-infrared spectral ranges," *Opt. and Spectrosc.,* **98** (4), 2005 (in press).